JOURNAL OF APPLIED ELECTROCHEMISTRY 19 (1989) 195–202

Transient regime in a parallelepipedic cell induced by a current or a potential step

F. LAPICQUE, J. M. HORNUT*, A. LOUCHKOFF, A. STORCK

Laboratoire des Sciences du Génie Chimique, CNRS-ENSIC-INPL, 1 rue Grandville, BP 451, F-54001 Nancy Cedex, France

Received 22 March 1988; revised 10 July 1988

On the basis of previous studies dealing with laminar flow in a channel electrode reactor, this work concerns the transient regime in a parallelepipedic cell induced by a current or a potential step for various types of flow. The response was shown theoretically to be governed by the wall velocity gradient. Experiments conducted in a rectangular cell provided with either flat or porous electrodes confirm the results of the model. Assuming a reversible electrochemical process, the transient behavior of a parallelepipedic cell can therefore be predicted through hydrodynamic and mass transfer data.

Nomenclature

b	channel depth (m)
C	concentration (mol m^{-3} or M)
D	diffusion coefficient (m^2 s^{-1})
d_h	hydraulic diameter (m)
E	electrode potential (V)
F	Faraday's constant
$f/2$	friction factor defined as $\tau_p/\varrho u_m^2$
i	current density (A m^{-2})
I	current (A)
I_L	limiting current (A)
k_d	mass transfer coefficient (m s^{-1})
L	electrode length (m)
m	function introduced by Aoki [2]
Re	Reynolds number in the empty channel
s	wall velocity gradient (s^{-1})
Sc	Schmidt number
Sh	Sherwood number in the empty channel
t	time (s)
T	temperature (K)
t_2	time required for the current to decrease down to twice the steady-state current, following a step of potential (s)
u	local fluid velocity (m s^{-1})
u_m	mean superficial velocity (m s^{-1})
w	channel width (m)
x	axial coordinate (m)
X	axial reduced coordinate
x_0	distance separating the edge of the channel and the electrode
y	coordinate in the normal direction to the electrode (m)
Y	reduced y coordinate (relation 34)
η	overpotential (V)
θ	reduced time
θ_2	reduced time corresponding to t_2
ν	kinematic viscosity (m^2 s^{-1})
ν_e	number of electrons involved in reaction
τ_p	wall shear stress (N m^{-2})

Subscripts

A, B, j	compound
b	bulk
e	electrode
0	standard
t	turbulent

1. Introduction

Parallelepipedic electrochemical reactors are frequently used for both industrial applications and fundamental investigations; the hydrodynamics of such reactors are generally well defined and allow, for instance, the study of electrode reaction mechanisms or the measurement of the diffusion coefficient of an electroactive species.

On the other hand, numerous papers dealing with pulsed current generally consider small electrodes for which the pulsation frequency can be fairly high. The efficiency of electrical pulsations on the desired performance of a cell obviously depends on the development of the concentration gradient at the electrode during the pulse period. A first attempt at the investigation of an electrochemical reactor under electrical pulsation may consist of the observation of the transient reactor response induced by a current or a potential step. The determination of the duration of the transient regime makes it possible to select the values of pulse-on and pulse-off times as functions of a desired application; this period is therefore an important item of information for the comprehensive design of a pulsed electrochemical reactor.

The transient regimes of channel electrodes have been studied previously. In addition to the famous laws of Sand and Cottrell, more recent investigations, based on the assumption of a laminar regime in a

* Also at: IUTB, Université de Nancy I, Le Montet, F-54600-Villers Les Nancy, France.

0021-891X/89 $03.00 + .12

parallelepipedic electrolyzer, have taken into account the convective term in the expression for the mass balance in the diffusional layer. On the basis of the redox reaction $A + v_e e \rightarrow B$, all authors have assumed that the solution did not contain B before electrolysis. Some authors considered current steps larger than the limiting current I_L [1, 2]; the values of transition times, τ, were measured or obtained through calculation and then compared to the corresponding values given by the Sand law, τ_0. Also, Compton *et al.* [3, 4] studied the variation of the cell current after a potential step: the time required for the establishment of the diffusional boundary layer was observed to be as much longer when the electrode is large and when the average fluid velocity is low.

The present paper deals with chronopotentiometric and chronoamperometric studies of a parallelepipedic reactor provided with flat or porous electrodes corresponding to preparative electrochemistry. The models developed in previous papers [2–4] can be generalized to a solution containing both species A and B flowing in the laminar or turbulent regime. The theoretical variations of the cell current or the electrode potential can be deduced through the hydrodynamics investigated previously. Theory and practice are shown to be in satisfactory agreement.

2. Theory

This part is dedicated to the generalization of the models presented by Aoki and by Compton. Consider a simple redox electrode reaction $A + e \rightarrow B$ in a single phase medium containing both dissolved species A and B. The model relies upon the following assumptions: (i) due to a large excess of supporting electrolyte, the effect of migration may be neglected; (ii) the counter electrode faces the working electrode; the electrolytic cell is defined by its channel depth, b, and by its width, w; the hydrodynamic regime may be laminar or turbulent; in addition, the flow is assumed to be fully established; (iii) the electrode length L is much larger than the diffusion layer thickness and the mass balances can be written neglecting the contribution of axial diffusion; (iv) the electrochemical reaction is reversible and the electrode potential can be expressed by the Nernst equation; (v) diffusion coefficients of species A and B have identical values.

Under the above assumptions, the convective–diffusion equation describing the concentration of compound j is:

$$\frac{\partial C_j}{\partial t} = D \frac{\partial^2 C_j}{\partial y^2} - u \frac{\partial C_j}{\partial x} \qquad (1)$$

where u is the axial flow velocity, which varies with the transverse coordinate y starting from the electrode surface. However, in the case of turbulent flow, the actual concentration and fluid velocity are the sum of an average component and a fluctuating component, which characterizes the extent of turbulence in the medium:

$$C_j = \bar{C}_j + \tilde{C}_j \quad \text{and} \quad u = \bar{u} + \tilde{u}$$

Thus, the convective–diffusion equation relative to non-laminar flow involves both average and fluctuating concentrations and velocity [5]. A turbulent diffusion coefficient can be introduced as a function of $(\tilde{C}_j \tilde{u})$ yielding another expression for the mass balance, very similar to expression 1

$$\frac{\partial \bar{C}_j}{\partial t} = (D + D_t) \frac{\partial^2 \bar{C}_j}{\partial y^2} - \bar{u} \frac{\partial \bar{C}_j}{\partial x} \qquad (2)$$

For the sake of simplicity, C_j and u will denote, respectively, the time-averaged component of concentration and velocity in the following text.

In liquid flow for which the Schmidt number is greater than or equal to 10^3, the thickness of the diffusion boundary layer is generally lower than the laminar sublayer thickness. Therefore, the velocity profile can be linearized by the relation $(u = sy)$ if s denotes the wall velocity gradient $(\partial u/\partial y)_{y=0}$; in addition D_t will be neglected in the mass balance 2. In a rigorous treatment, this assumption has to be verified for the actual flow conditions.

Following previous derivations, dimensionless variables can be defined as:

$$X = x/L, \quad Y = y(sL^{-1}D^{-1})^{1/3}$$

and

$$\theta = t(Ds^2L^{-2})^{1/3} \qquad (3)$$

Equation 2 is therefore expressed in the reduced form:

$$\frac{\partial C_j}{\partial \theta} = \frac{\partial^2 C_j}{\partial Y^2} - Y \frac{\partial C_j}{\partial X} \qquad (4)$$

The transient response induced by a potential step or a current pulse is governed by the wall velocity gradient and thus by the hydrodynamics in the cell. We now examine the techniques for the determination of the velocity gradient before describing the solution of Equation 4 for chronopotentiometric or chronoamperometric studies in the reactor.

2.1. *Estimation of wall velocity gradient*

In a general manner, the magnitude of the wall velocity gradient depends on local physical conditions; thus the time required for establishment of the diffusion layer can be a function of electrode surface coordinates x and z. However, to a first approximation, one can consider s values averaged over the entire electrode surface, yielding an overall transient response of the reactor. This gradient can be reached by several methods.

At first, s can be obtained through an analytical derivation of the expression for the velocity profile. Provided a well-established laminar flow exists in the reactor, the velocity profile is parabolic if edge effects are negligible, i.e. if $b \ll w$; the corresponding velocity gradient equals $(6u_m/b)$. Edge effects have to be taken into account if the electrode fills the whole channel width or if w and b are of the same order of magnitude. The laminar velocity profile is therefore a function of the three spatial coordinates x, y and z. For liquid

flowing in the transition or turbulent regime, the existence of a laminar sublayer at the vicinity of the electrode is frequently assumed. Blasius [6] proposed an 'exact' solution for the velocity profile in the sublayer which is valid for a well-established turbulent regime in the bulk. The derived expression for s is a function of the axial coordinate x (Table 1).

When the expression for the velocity profile is not directly available, the value of s can be reached by measuring the limiting current on a microelectrode inserted into a non-conducting wall [7, 8].

Another possibility relies upon mass and momentum transfer analogies: values of the friction factor, $f/2$, are therefore deduced from mass transfer rate formerly determined and s can be expressed as a function of friction factor $f/2$ through the wall shear stress τ_p.

$$s = f/2 \frac{u_m^2}{\nu} \tag{5}$$

Several correlations express the analogy of mass and momentum transfer near a flat solid wall in a channel reactor. Their accuracy fairly depends on the complexity of the hydrodynamics and the models proposed by Lin *et al.* [9] and Sandall *et al.* [10] are known to provide satisfactory results for fully turbulent flow in the case of high Schmidt values. These expressions for mass and momentum transfer analogy are reported in Table 1.

For more complex systems such as porous electrodes, classical correlations such as the well-known relation of Calderbank and Moo-Young [11] can provide estimated values for s. Nevertheless, after this relation, mass transfer coefficient varies with $s^{0.25}$, and its use may involve significant errors in the resulting values of s; more accurate values should be obtained through pressure drop measurements in the reactor to yield the magnitude of the friction factor.

2.2. *Electrode potential step* [3, 4]

The variations of concentration profile at the vicinity of the electrode can be obtained through integration of Equation 4 taking into account the boundary conditions:

$$\begin{array}{lll} \theta = 0 & Y \geqslant 0 & C_j = C_{jb} \\ \theta > 0 & Y \to \infty & C_j \to C_{jb} \\ \theta > 0 & Y = 0 & C_j = C_{je} \end{array} \tag{6}$$

where C_{jb} and C_{je} are the concentration in the bulk and at the electrode, respectively. The C_{je} value is a function of the electrode potential E and is time invariant. Compton *et al.* solved Equation 4 subjected to conditions 6 making use of a double Laplace transform and numerical techniques to accelerate the convergence of the series in the Laplace domain. The ratio of the cell current and the steady-state current (I/I_∞) was then computed as a function of reduced time θ. The obtained variation, expressed in a dimensionless form, seems to be valid whatever the hydrodynamic flow and whatever the substrate concentration at the electrode. Above all, θ_2 is defined as the time required for the current to decrease from its initial value to twice the final steady-state value; θ_2 was found to be close to 0.35.

Table 1. Expressions for $f/2$ as function of the fluid velocity and the mass transfer coefficient for a turbulent flow in rectangular channel

Reference	*Correlation*
[6]	$f/2 = \frac{1}{L}\int_{x_0}^{x_0+L} 0.332 \left(\frac{\nu}{u_m x}\right)^{1/2} dx$
[9] (approx. relation)	$\frac{k_d}{u_m} = \frac{f/2}{1 + 14.24(Sc^{0.685} - 1)\sqrt{f/2}}$
[10]	$\frac{k_d}{u_m} = \frac{\sqrt{f/2}}{A + 2.78 \ln [(Re\sqrt{f/2})/90]}$ where $A = 12.48Sc^{2/3} - 7.853Sc^{1/3} + 3.613 \ln(Sc)$

2.3. *Current step* [2]

At time $t = 0$, the closure of the electrical circuit applies to the reactor a constant current I; I can be lower or larger than the steady-state limiting current, I_L. The boundary conditions 6 are still valid but C_{je} now varies with time. Additional boundary conditions are required:

$$\begin{gathered} \theta > 0 \qquad 0 < X < 1 \qquad Y = 0 \\ D(\partial C_A/\partial y) = -D(\partial C_B/\partial y) = i(t, x)/\nu_e F \\ E(t) = E_0 + (RT/\nu_e F) \ln (C_{Ae}/C_{Be}) \end{gathered} \tag{7}$$

as a Nernstian redox electrochemical process is assumed. Finally, the condition for chronopotentiometric electrolysis is written as:

$$I = w \int_0^L i(t, x)\, dx \tag{8}$$

A double Laplace transform is applied to differential Equation 4 with respect to X and θ and, as done by Aoki *et al.*, surface concentrations can be correlated to the bulk concentrations:

$$C_{Ae} + C_{Be} = C_{Ab} + C_{Bb} \tag{9}$$

From Equations 7 and 9 it can be deduced that surface concentrations are solely functions of reduced time and the function $m(\theta)$ is therefore introduced as:

$$\begin{aligned} C_{Ae} &= C_{Ab}[1 - (I/I_L)m(\theta)] \\ C_{Be} &= C_{Bb} + C_{Ab}(I/I_L)m(\theta) \end{aligned} \tag{10}$$

m is an increasing function with time and can be calculated [2]. The equation for the electrode potential yields:

$$E = E_0 + \frac{RT}{\nu_e F} \ln \left[\frac{1 - (I/I_L)m(\theta)}{C_{Bb}/C_{Ab} + (I/I_L)m(\theta)} \right] \tag{11}$$

As a function of the order of magnitude of both bulk concentrations, two limiting situations may be

encountered:

$$^{*}C_{Bb} \gg C_{Ab}$$

$$E \sim E_0 + \frac{RT}{vF} \ln \frac{C_{Ab}}{C_{Bb}} + \frac{RT}{v_e F} \ln \left[1 - \frac{I}{I_L} m(\theta) \right]$$

or

$$E \sim E_0' + \frac{RT}{v_e F} \ln \left[1 - \frac{I}{I_L} m(\theta) \right]$$

$$^{*}C_{Bb} \ll C_{Ab} \qquad E \sim E_0 + \frac{RT}{vF} \ln \left[\frac{1 - (I/I_L)m(\theta)}{(I/I_L)m(\theta)} \right]$$

The electrochemical reactor has to be characterized in terms of hydrodynamics and mass transfer prior to investigations of its transient response.

3. Description of the reactor, hydrodynamics and mass transfer

3.1. *Description of the reactor*

The vertical cell is divided into two symmetrical compartments by means of an Ionac® membrane. A Pt wire fixed on the reactor outlet acts as a reference electrode. Both electrolytic compartments have dimensions of 5 × 40 × 85 mm. The electrolyte is distributed at the bottom by a fixed bed of 3 mm diameter glass spheres acting as a calming zone; this device allows appreciable reduction of the turbulence generated by the change in flow direction (Fig. 1). Due to the reactor dimensions, the wall velocity gradient could not be measured with the help of microelectrodes in non-conducting wall and was evaluated from the mass transfer rate at the electrode. The electrodes are fixed at a distance x_0 equal to 35 mm above the higher edge of the fluid inlet (Fig. 1). Electrodes can be removed from the reactor and two different cell designs were considered: (i) A channel electrolyzer with two carefully polished nickel electrodes whose dimensions are 40 × 60 mm. The fluid velocity was varied between 0.02 and 0.40 m s^{-1} and the corresponding Reynolds number was in the range 200–4000. (ii) A stack of three sheets of expanded platinized titanium made it possible to investigate the transient behavior of volumic electrodes. Such electrodes are well known to enhance the extent of turbulence. External dimensions of one sheet were 40 × 70 mm and the mesh had the following characteristic dimensions: long diagonal, 10.8 mm; short diagonal, 6.0 mm; metal sheet thickness, 0.85 mm and wire broadness 1.2 mm. The area of each of the two stacks – anode and cathode – was estimated to be close to 0.012 m^2. With regard to the orientation of the grid mesh, the large diagonal was disposed parallel to the electrolyte flow; in addition grids were placed in a perfect superposition in the reactor [12]. The stack porosity has been estimated to be approximately equal to 0.80 by comparison of the channel volume with the volume of expanded metal.

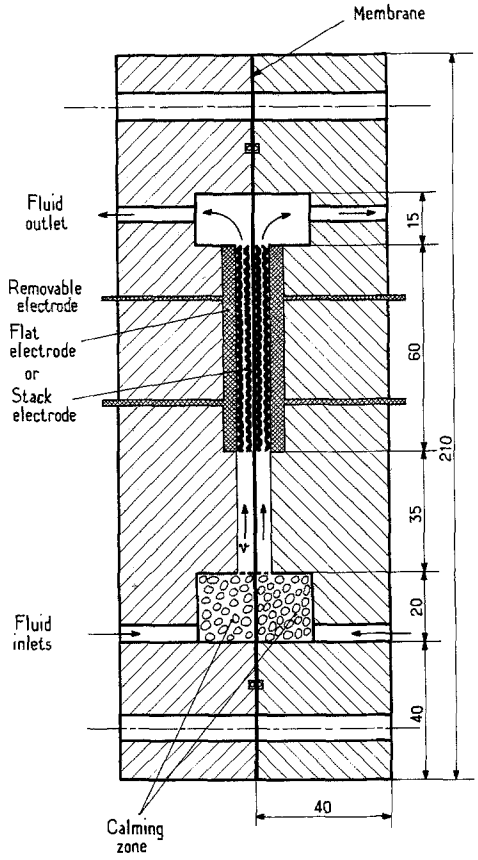

Fig. 1. Schematic view of the electrochemical reactor.

3.2. *Channel electrodes*

Mass transfer coefficients were determined by measurement of the limiting current for reduction of potassium ferricyanide. The electrolyte was a solution of 0.5 M NaOH containing potassium ferricyanide (5 × 10^{-3} M) and potassium ferrocyanide (0.10 M). Experiments were carried out at 20 ± 1 °C; at this temperature the kinematic viscosity, ν, and the diffusion coefficient of the electroactive species, D, are 0.90 × 10^{-6} and 8.8 × 10^{-10} m s^{-2}, respectively.

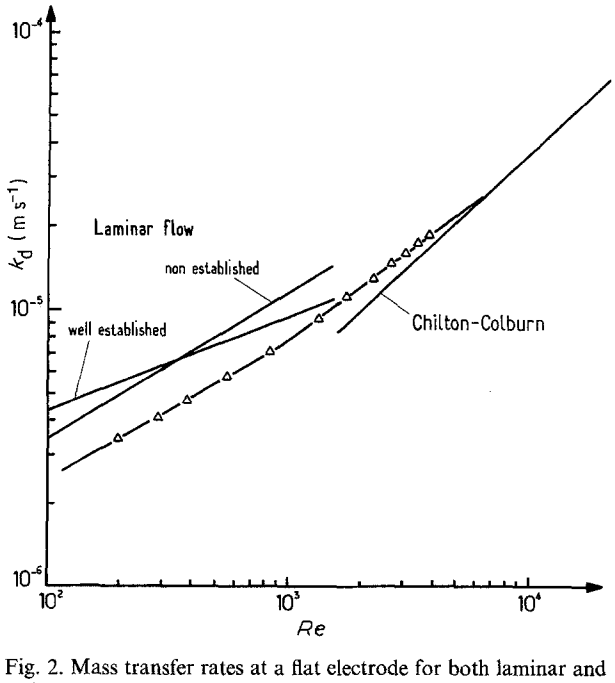

Fig. 2. Mass transfer rates at a flat electrode for both laminar and turbulent flows; comparison with literature data.

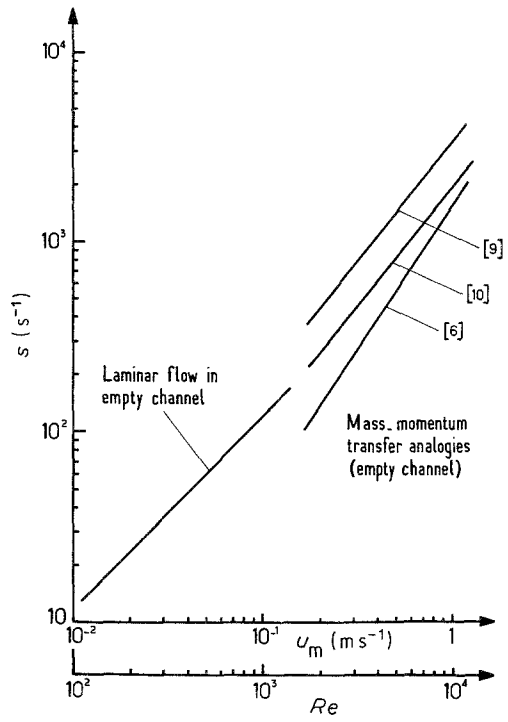

Fig. 3. Variation of the wall velocity gradient with superficial velocity for a flat electrode.

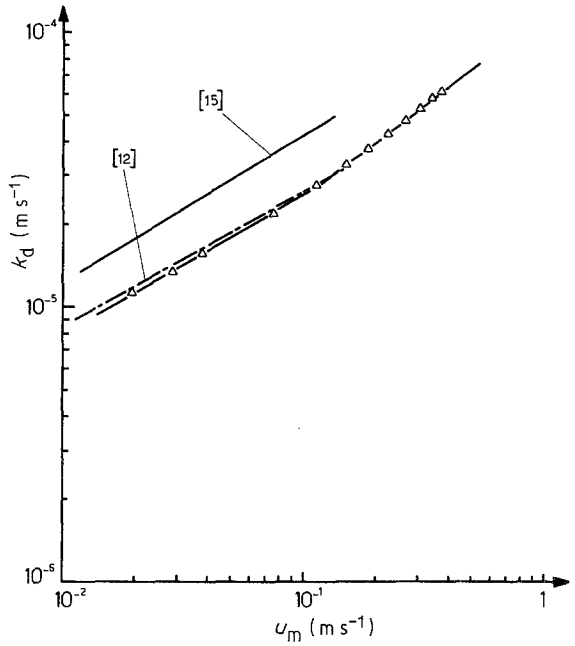

Fig. 4. Mass transfer coefficient at the stack electrode as a function of superficial velocity; comparison with literature data.

Nickel electrodes were activated by 10 min gas evolution periods: hydrogen at -1.5 V/SCE followed by oxygen evolution prior to another H_2 generation period.

Experimental values of mass transfer coefficient at the electrode are plotted versus the Reynolds number in Fig. 2. Due to the range of *Re* investigated, the plot obviously displays both laminar and turbulent hydrodynamics. Experimental results are in a fairly good agreement with literature data relevant to both laminar and turbulent flow; correlations considered are reported in Table 2. For fluid velocity below 0.1 m s^{-1}, corresponding to values of *Re* lower than 1000, k_d varies linearly with $u_m^{0.47}$. Despite the observed discrepancy between experimental results and literature data, the value of the exponent in u_m demonstrates a non-established laminar flow, which is probably due to the small distance between the electrodes and the edge at the fluid inlet. Increasing the velocity up to 0.3 or 0.4 m s^{-1} enlarges the turbulence intensity and k_d becomes proportional to $u_m^{0.66}$.

Estimated values of the wall velocity gradient in the cell are plotted in Fig. 3 versus the average fluid velocity and the Reynolds number: in the case of the laminar regime, edge effects were assumed to be negligible despite the reactor design. In addition, s values corresponding to a more turbulent flow were deduced from the relations given in Table 2 — even though flow is not fully turbulent for a Reynolds number of 4000 or so, and eventually from experimental values of mass transfer coefficient. The dependence on average flow velocity is more significant in turbulent flow for which the exponent of a power expression for s is close to 1.3 according to Lin or Sandall and is equal to 1.5 after Blasius. As a consequence of the small dimensions of the cell, s values up to 500 or 10^3 s^{-1} could be reached for a velocity of 0.4 m s^{-1}.

3.3. *Volumic electrodes*

As expected, mass transfer rates at the porous electrode are higher than the corresponding ones in an empty channel (Fig. 4). The variation of k_d with the superficial fluid velocity exhibits two regions (Fig. 4). Below 0.06 m s^{-1}, k_d is a linear function of $u_m^{0.4}$; increasing the turbulence at the expanded metal leads to a higher dependence on superficial flow velocity and k_d varies with $u_m^{0.7}$ in the range of velocity 0.2–0.4 m s^{-1}. Due to the large diversity of expanded metals, mass transfer performance cannot be compared directly

Table 2. Usual mass transfer correlations in a rectangular channel

Hydrodynamical regime	*Reference*	*Correlation*
Laminar well-established flow	[13]	$Sh = 1.467\left(\frac{2}{1 + b/w}\right)^{1/3}(ReScd_h/L)^{1/3}$
Laminar non-established flow	[14]	$\frac{k_d(x_0 + L)}{D} = 0.96\left[\frac{u_m(x_0 + L)}{\nu}\right]\left[Sc^{1/3}\frac{[1 - (x_0/L)^{3/4}]^{2/3}}{1 - x_0/L}(d_h/L)^{-0.05}\right]^{0.5}$
Turbulent well-established flow		$Sh = 0.023Re^{0.8}Sc^{1/3}$ (Chilton–Colburn)

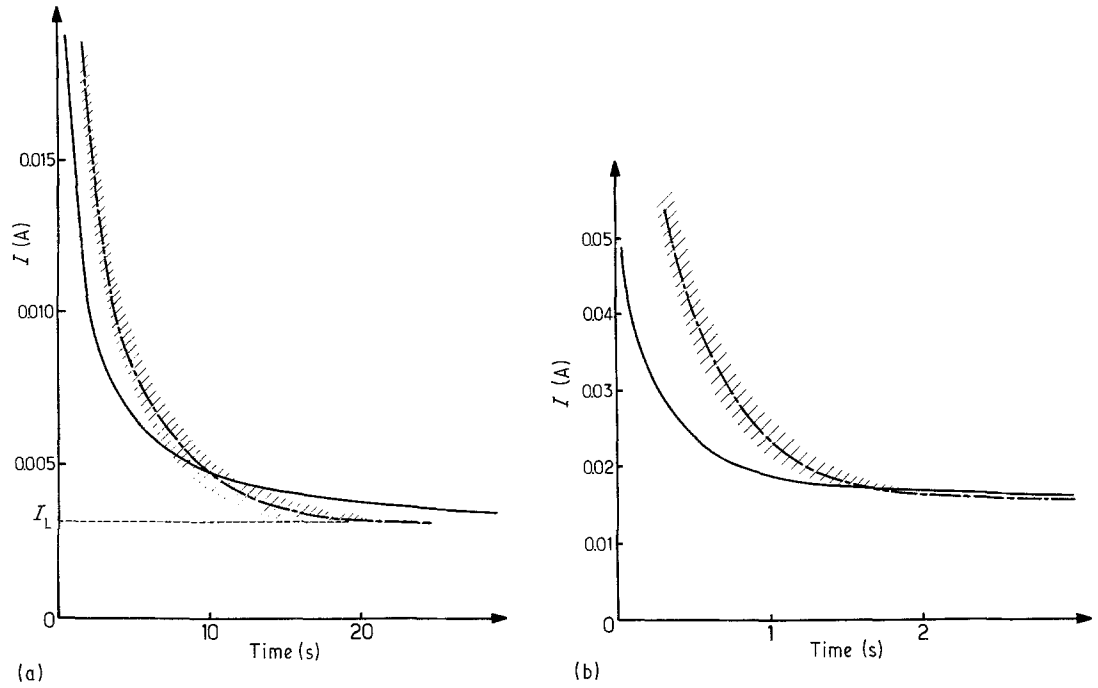

Fig. 5. Time variation of the current cell provided with flat electrodes; potential step = −300 mV (diffusion-controlled operation); (——) experiment (- - - and hatched zone) model and estimated values for s over the range ±20%. (a) $u_m = 0.0194\,m\,s^{-1}$ and $s = 6u_m/b$; (b) $u_m = 0.284\,m\,s^{-1}$ and s obtained through Lin's analogy.

with the results of previous studies [12, 15]. In addition these studies regard only fluid velocity below $0.15\,m\,s^{-1}$. Although a dimensionless correlation for such electrode materials was recently proposed [15], the comparison was discussed in terms of k_d vs u_m. A good agreement is observed between experimental data and results published by Leroux and Coeuret [12]; both series of values are 30% below values estimated from [15].

Values for the wall velocity gradient could not be calculated from mass transfer rates with satisfactory accuracy, using Calderbank's correlation. Thus, the transient response of this particular reactor could not be calculated.

4. Potential and current steps

Experimental responses were observed for the reduction of potassium ferricyanide. Nickel electrodes were activated in the same way as for previous experiments to determine mass transfer performances in the reactor.

Both current and potential steps were generated by a square signal Tacussel GSTP3 device. Cell current was delivered by a Tacussel PRT 20-2 potentiostat and the cell transient response (potential or current) was continuously registered by means of a chart recorder. In the case of chronopotentiometric experiments, measuring the transient electrode potential led to time variation of the overpotential η. The electric device — step generator and electric supply — has a response time below 10^{-3} s and the accuracy of the sampling of cell response is solely affected by the recorder. Therefore, the error involved in the measurement of the characteristic time t_2 was estimated to 0.1 s or so.

4.1. *Potential steps*

Two values of electrode overpotential have been considered: −300 mV, corresponding to limiting current and −20 mV, for which the electrolytic reduction is ruled by both diffusion and activation. As expected from former studies, the cell current decreases from a very high value to its steady-state value. As a function of the flow velocity, the time required for the current decay at a channel electrode varies from 1 to 30 s or so. Moreover, the transient phenomenon occurs within only 1 s in a porous electrode reactor.

Calculated variations of the cell current can be obtained from Compton's results [3], using estimated values for s and mass transfer rates at the electrode. Experimental and theoretical variations exhibit similar decays and steady-state currents (Fig. 5). Nevertheless, experimental variations are generally twice faster than predicted ones: the observed discrepancy might stem from errors in s values estimated through mass and momentum transfer analogies. In order to assess the sensitivity of this treatment, the value of the wall velocity gradient was varied over a range (±20%), corresponding to the error estimate for s determination, and the analysis repeated. As reduced time varies with $s^{2/3}$, the s range investigated corresponds to a time deviation close to ±13% for a fixed current value; Fig. 5 seems to show that the model sensitivity with s cannot explain the observed discrepancy, and another explanation has to be suggested.

Characteristic times, t_2, were deduced from current variations and their dependence on flow velocity is reported in Figs 6 and 7. For the example of channel electrodes in a laminar or a fairly turbulent regime, the comparison with predicted values is possible from the

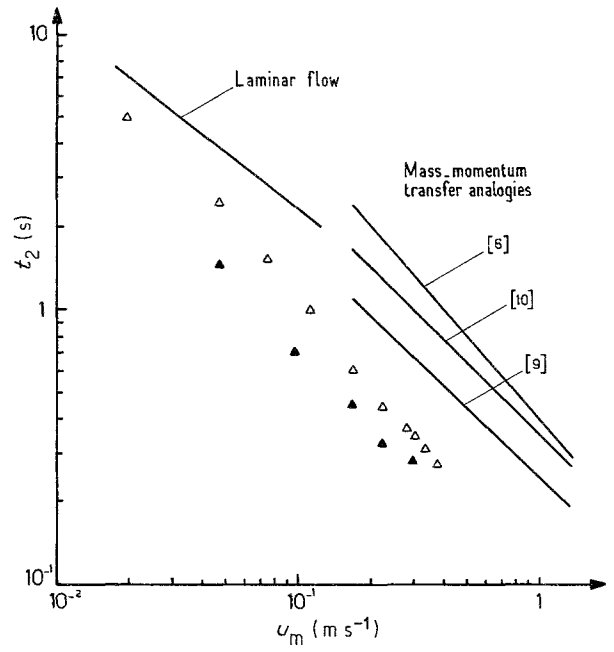

Fig. 6. Variation of characteristic time t_2 with superficial velocity at a channel electrode; (Δ) experimental results for $\eta = -300$ V; (Δ) experimental results for $\eta = -20$ mV; comparison with theory assuming that $\theta_2 = 0.35$ after [3].

value for dimensionless time, θ_2, after Compton. In the case of a channel electrode, experimental results are well below predicted times, t_2, for both laminar and turbulent flow. In addition, contrary to the results of the model, the decays recorded for $\eta = -20$ mV are 20–30% faster than the corresponding ones relative to a diffusion controlled operation. The presence of grids increases the extent of turbulence at the electrode, corresponding to enhanced s values; as a consequence, transient decrease of the cell current occurs within very short times.

4.2. *Current steps*

Experiments were conducted for various values of the ratio I/I_L. The aim of this part does not concern the experimental determination of the transition time τ, but the measurement of the time variation of the electrode potential in the case of one electrochemical process. Hence only values for I/I_L lower than unity were considered.

As observed for chronoamperometric experiments, the time required for a steady-state potential is a decreasing function of the fluid velocity (Figs 8 and 9). Theoretical η variations were deduced from expression 11 and the numerical values for function $m(\theta)$ [2], taking into account the chemical composition of the electrolyte. Theory and practice have to be compared with regards to both steady-state overpotential and kinetics of electrode potential variation. Due to the activation procedure of the nickel electrodes, the reduction can be assumed to be a Nernstian electrochemical process as experimental overpotentials at steady-state conditions are fairly close to corresponding predicted values (Fig. 8). In addition, calculation and experimental approach for a channel electrode

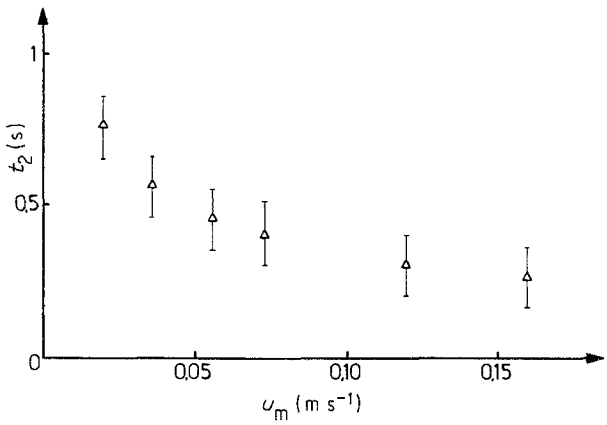

Fig. 7. Experimental variation of characteristic time t_2 with superficial velocity at a stack electrode; $\eta = -300$ mV.

reactor yield very similar overpotential variations, thus confirming the model presented above.

5. Conclusion

The models for the transient response of a parallelepipedic electrochemical reactor proposed by Aoki and Compton in restrictive conditions can be simply enlarged to more general operational modes. As an example, turbulent flow can be considered. The transient operation of a reactor was found to be solely dependent on hydrodynamics at the electrode, characterized by the wall velocity gradient, and on the chemical composition of bulk electrolyte. On the basis of an electrochemical reactor provided with either flat or porous electrodes, experimental variations of the current cell or its electrode overpotential validate the assumptions and the results of the model described. For a reversible electrochemical process, the transient behavior of a parallelepipedic cell can simply be predicted through hydrodynamic and mass transfer data.

Current pulsations can be considered as the sequence of positive and negative current steps. Therefore the results of the present work allow order of magnitude for pulse-in and pulse-off times and a pulsed electrochemical process in a rectangular cell to be carried out in a comprehensive manner. Nevertheless, the electric response of a system induced by a single step differs slightly from its behavior under current or potential pulsations and this research theme has to be investigated for parallelepipedic cells.

Acknowledgements

The present work was partly sponsored by financial support from the 'Programmes Interdisciplinaires de Recherches sur les Sciences pour l'Energie et les Matières Premières' of the 'Centre National de la Recherche Scientifique'.

References

[1] F. A. Posey and R. E. Meyer, *J. Electroanal. Chem.* **30** (1971) 359.

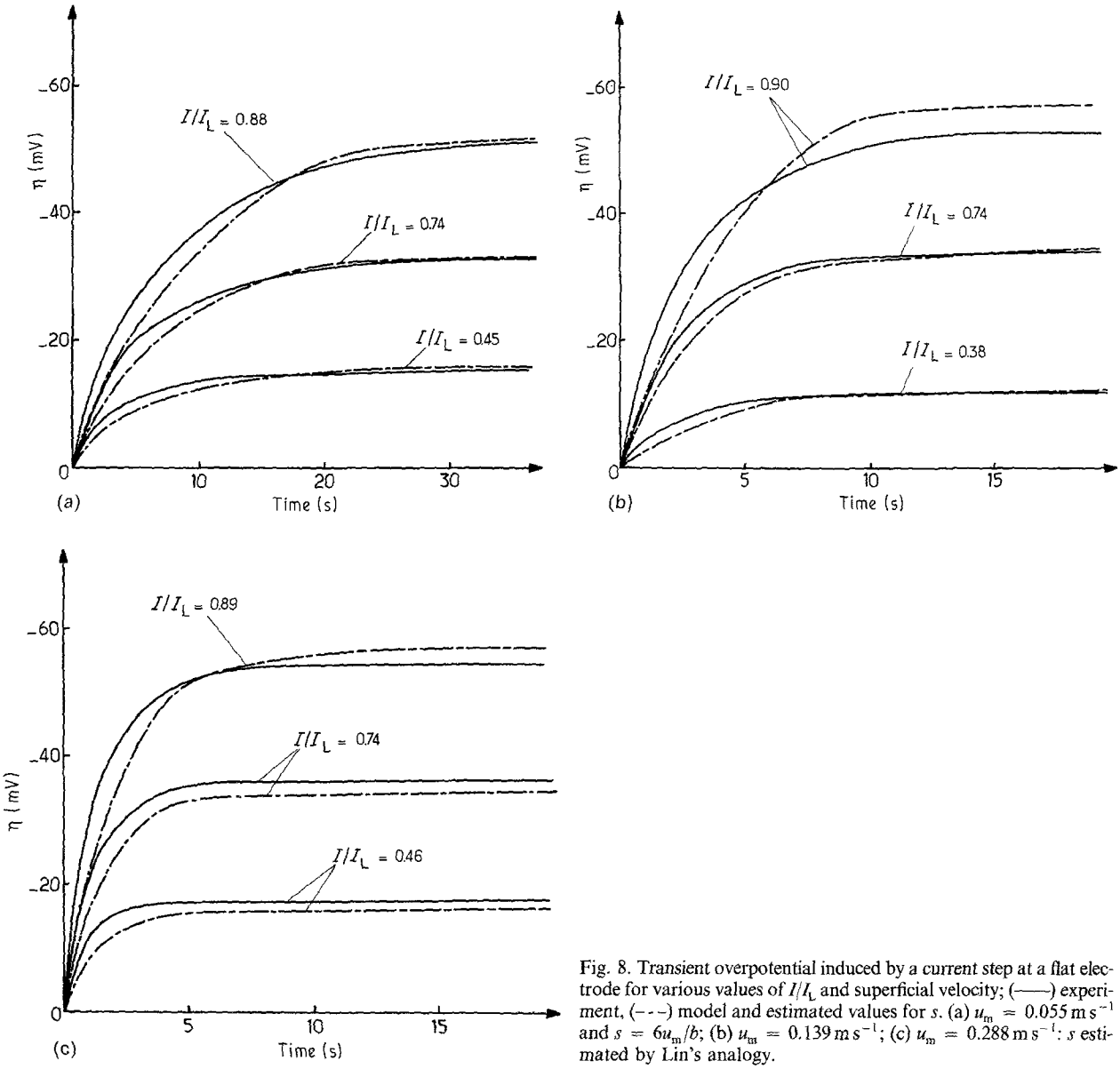

Fig. 8. Transient overpotential induced by a current step at a flat electrode for various values of I/I_L and superficial velocity; (——) experiment, (- - -) model and estimated values for s. (a) $u_m = 0.055\,m\,s^{-1}$ and $s = 6u_m/b$; (b) $u_m = 0.139\,m\,s^{-1}$; (c) $u_m = 0.288\,m\,s^{-1}$: s estimated by Lin's analogy.

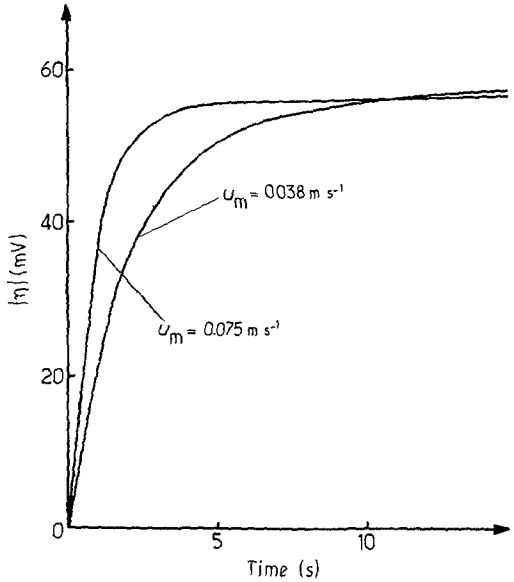

Fig. 9. Experimental transient overpotential induced by a current step ($I/I_L = 0.88$) at a stack electrode for two values of superficial velocity.

[2] K. Aoki, K. Tokuda and H. Matsuda, *J. Electroanal. Chem.* **175** (1984) 1.
[3] R. G. Compton and P. J. Daly, *J. Electroanal. Chem.* **178** (1984) 45.
[4] R. G. Compton and P. R. Unwin, *J. Electroanal. Chem.* **205** (1986) 1.
[5] V. G. Levich, 'Physico-chemical Hydrodynamics', Prentice Hall, Englewood Cliffs, NJ (1958); N. Midoux, 'Mécanique et Rhéologie des fluides en Génie Chimique', Technique et Documentation, Lavoisier, Paris (1985).
[6] H. Blasius, *Z. Math. Phys.* **56** (1908) 1.
[7] A. Storck and F. Coeuret, *Electrochim. Acta* **22** (1977) 1155.
[8] F. Giron, G. Valentin, M. Lebouche and A. Storck, *J. Appl. Electrochem.* **15** (1985) 557.
[9] C. S. Lin, E. B. Denton, H. L. Gaskill and G. L. Putnam, *Ind. Eng. Chem.* **43** (1951) 2136.
[10] O. C. Sandall, O. T. Hanna and P. R. Mazet, *Can. J. Chem. Eng.* **58** (1980) 443.
[11] P. H. Calderbank and M. Moo-Young, *Chem. Eng. Sci.* **16** (1961) 39.
[12] F. Leroux and F. Coeuret, *Electrochim. Acta* **30** (1985) 159.
[13] D. J. Pickett and B. R. Stanmore, *J. Appl. Electrochem.* **2** (1972) 151.
[14] D. J. Pickett and K. L. Ong, *Electrochim. Acta* **19** (1974) 875.
[15] S. Piovano and U Böhm, *J. Appl. Electrochem.* **17** (1987) 123.